

MnS Hierarchical Hollow Spheres with Novel Shell Structure

Yao Cheng, Yuansheng Wang,* Chong Jia, and Feng Bao

State Key Laboratory of Structural Chemistry, Fujian Institute of Research on the Structure of Matter, Chinese Academy of Sciences, Graduate School of Chinese Academy of Sciences, Fuzhou, Fujian 350002, China

Received: June 14, 2006; In Final Form: September 22, 2006

High yields of MnS microspheres with novel hierarchical structure were prepared through a simple solution method. Field emission scanning electron microscopy and transmission electron microscopy analyses reveal that the microsphere has a core–shell structure: the interior hollow sphere is covered by a shell consisting of nanorod arrays. Interestingly, the nanorod is a wurtzite (WZ)/zinc blende (ZB) phase admixture with a large amount of stacking faults/twins. The alternation of WZ and ZB along the growth direction of the nanorod enables it to exhibit the features of a quantum well. Furthermore, the WZ/ZB admixture structure could also be regarded as a type II homomaterial heterostructure. All these features imply that the novel core–shell structure has great potential for applications, among them the quantum well photoelectrical and heterostructure photoconduction fields.

Introduction

The past few years have witnessed increasing attention focused on the novel structures of inorganic materials from nanoscale to microscale size, including one dimensional, hollow, and hierarchal structures, because of their unique structure-induced optical, electrical, and surface properties that may bring a series of opportunities for their potential applications as photoelectric devices, drug delivery, sensors, filters, coatings, and chemical catalysis.^{1–4} Considerable progress has been made in the synthesis of some well-known structures, such as rods,⁵ belts,³ hollow spheres,⁶ tubes,⁷ dendrites,⁸ and cages.⁹ Specific structural characteristics may correspond to distinct performance specialties. From this point, one would expect that the combination of more than one structural characteristic within a single material or that the increase of the structural complexity of the material may realize the invention of some unique physical and chemical properties. Each of these characteristics may relate to an individual structural characteristic or even bring unexpected novel properties and thus enable the materials to meet more of the needs of technology. As expected, contemporary chemists and material scientists seem unsatisfied with these somewhat simple structures, and many efforts have been devoted to constructing complex structural admixtures. For example, a dandelion-like conformation with hollow interiors had been fabricated for CuO¹⁰ and ZnO,¹¹ and the unique structural features of one- or two-dimensional anisotropic building blocks aligned into highly symmetrical isotropic three-dimensional conformations may find potential application in three-dimensional lasing. The successful synthesis of an amorphous calcium carbonate hollow spherical superstructure provided a precursor for the construction of the novel morphology of crystalline CaCO₃.⁴ The rhombododecahedral silver cages with a multilevel superstructure could be used as a model for the understanding of biological minerals.¹²

As a p-type semiconductor with a wide gap ($E_g \approx 3.7$ eV), manganese sulfide (MnS) has potential application in solar cells as a window/buffer material. In addition, it is also linked with

the study of diluted magnetic semiconductors (DMS). In recent years, particularly, stimulated by the application of Mn doping DMS in blue/green light emitters¹³ and the discovery of colossal magnetoresistance in Fe_{1-x}Mn_xS solid solutions,¹⁴ investigations concerning pure Mn chalcogenides were revived. MnS is known to crystallize into three different polymorphs: the rock salt structure (α -MnS), the zinc blende structure (β -MnS), and the wurzite structure (γ -MnS). As some reports^{15–17} about different polymorphs with specific morphology came forth, interest has been focused on the control of the morphology/structure of MnS. A few months ago, we demonstrated that metastable γ -MnS core–shell hollow spheres could be obtained through a solvothermal route in ethylene glycol (EG) solvent.¹⁸ Herein, as a continued work, we report that by simply replacing the solvent, another novel hierarchical structure of γ -MnS, which combines hollow interior features with nanorod arrays characteristic of the shell, is presented. The structural analysis revealed that there are large amount of stacking faults/twins existing throughout each nanorod, resulting from the wurtzite (WZ)/zinc-blende (ZB) phase admixture. Furthermore, the alternation of WZ/ZB structure could be regarded as a type II homomaterial heterostructure, which enables the material promising applications in the fields of photoelectricity and photoconduction.

Experimental Section

The synthesis of γ -MnS semiconductor hierarchical hollow spheres proceeded through a solvothermal route. Manganese acetate, sulfur powder (S), poly(*N*-vinyl-2-pyrrolidone) (PVP, $M_w = 30\,000$), and *N,N*-dimethylformamide (DMF) were all of AR grade and purchased from Shanghai Chemical Reagent Ltd., China; these were used as starting materials. In a typical synthesis procedure, 0.245 g (1 mmol) of metal acetate and 0.500 g (2×10^{-5} mmol) of PVP were dissolved in 12 mL of DMF, and the mixture was then transferred to a Teflon-lined stainless steel autoclave of 20 mL capacity followed by the addition of 0.032 g (1 mmol) of sulfur. The sealed tank was heated at a rate of 5 °C/min to 180 °C, maintained at this temperature for 12 h in an oven, and then allowed to cool to room temperature. The resulting precipitates were collected by

* Corresponding author. Tel/fax: +86-591-8370-5402. E-mail: yswang@fjirsm.ac.cn.

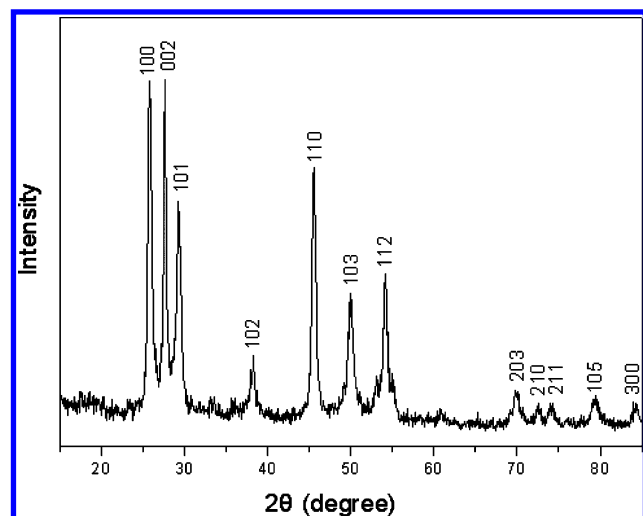


Figure 1. XRD pattern of the sample synthesized at 180 °C for 12 h.

centrifugation, washed with CS₂ and pure ethanol several times, and finally air-dried.

Powder X-ray diffraction (XRD) patterns of the synthesized samples were recorded by X-ray diffractometer (RIGAKU-DMAX2500) with Cu K α radiation ($\lambda = 0.154$ nm) at a scanning rate of 5°/min for 2θ ranging from 5° to 85°. The morphology and microstructure of the samples were characterized by the transmission electron microscope (TEM, JEOL-2010) operated at 200 kV and by the field emission scanning electron microscope (SEM, JSM-6700F) working at 10 kV.

Results and Discussion

The XRD pattern of the prepared pink sample shown in Figure 1 could be indexed to MnS wurtzite phase (space group, $P6_3mc$; JCPDS card no. 40-1289), with the lattice constants a and c as 0.3990 and 0.6453 nm, respectively. Figure 2a shows the general morphologies of the prepared MnS products, which confirms a nearly 100% yield of the microspheres with the diameter distributed from 1.5 to 3.0 μm . Detailed observation of the surface of an individual microsphere reveals that it is constructed by nanorod arrays and that the diameter of the nanorods ranges from 25 to 50 nm, as shown in Figure 2b. The hierarchical and hollow structural characteristics of the MnS microspheres were further exposed by FESEM imaging of the cracked spheres, as shown in parts c and d of Figure 2. One can also clearly recognize a hollow sphere consisting of nanocrystals beneath the nanorod arrays. Although the hollow and core-shell structures have been reported for many materials, the combination of them in one object is quite novel and may bring new opportunity for material applications.

The structural characterization and the hierarchical nature of the MnS microspheres were further examined by TEM and high-resolution TEM (HRTEM) observations. As shown in Figure 3a, in agreement with the above SEM results, the abrupt core-shell transition and the inner cavity of the microspheres are clearly revealed by the changes in contrast. One of the HRTEM observations and its corresponding fast Fourier transform (FFT) pattern are shown in Figure 3e, revealing that the nanorod grows preferentially along its c -axis, which, for the wurtzite structure, implies a chemical bipolarity of the rod, with one tip covered by a plane of S atoms and the other by a plane of Mn atoms. In our previous work,¹⁸ it was demonstrated that the MnS core-shell hierarchical hollow structure was achieved via Ostwald ripening; namely, the core substances dissolved into the solution while the secondary nucleation of the crystalline polymorph

occurred on the external surface. Incidentally, it was also observed that some tiny, irregular nanorods existed in the shell, which inspired us to further modify the core-shell structure; e.g., to develop the rod structure in the shell while preserving the core-shell characteristic. However, with EG as the solvent, the nanorods in the shell were always poorly developed. They were very short and irregularly shaped and in some cases did not appear at all. Therefore, the main difference resides in the manner with which the secondary nucleation on the external surface was adopted. It was believed that metal chalcogenides with wurtzite structures could preferentially develop along their unique c -axes in the presence of suitable surfactants, since the lateral nonpolar facets have much lower growth rates than the basal polar facets.¹⁹ In the present case, the solvent DMF acts as a more suitable surfactant than EG for the anisotropic growth of wurtzite MnS during the secondary nucleation on the external surface of the microsphere, resulting in the formation of nanorod arrays in the shell.

From the enlarged TEM micrographs of the local nanorod array shown in Figure 3b, it is evident that every nanorod exhibits a strong wavy diffraction contrast at the top, which is related to plane defects.²⁰ The HRTEM image taken from the squared region of Figure 3b, shown in Figure 3c, confirms the presence of densely distributed stacking faults/twin planes perpendicular to the growth direction. Further examinations of the rods broken off from the sphere reveal that such wavy contrast (stacking faults/twins) exists across the entire rod, as indicated by Figure 3d. The HRTEM image from an individual nanorod, as shown in Figure 3e, exhibits a large amount of (0001) stacking faults/twin planes. In the corresponding FFT pattern inserted in Figure 3e, the reflections in the series are almost linked with each other to form bright lines in the direction along the c -axis, as a result of the consecutive reflection splittings induced by the dense plane defects. Further analysis of the HRTEM image and of the corresponding FFT patterns demonstrates that the nanorod is actually a mixture of wurtzite and zinc blende, as illustrated in Figure 3I and 3II, where the stacking fault and the twin are labeled by "SF" and "twin", respectively. From the structural point of view, different basal-plane stacking sequences lead to distinct lattice structures: a stacking sequence of ABAB along the [001] direction forms a hexagonal phase, whereas one of ABCABC along the [111] direction results in a cubic phase. The two structures could be transformed reversibly; i.e., an alternate transformation between the (001) plane of WZ and the (111) plane of ZB could be created by simply changing the stacking sequence. Considering the particular crystallographic characteristics of the two polymorphs, two types of transformation mechanisms have been proposed.³ One involves the rearrangement of three basal layers, leading to (111) twinning in zinc blende. The other involves the rearrangement of four basal layers, inducing the generation of stacking faults. Similar phenomena have been observed in a few binary chalcogenide systems, such as CdSe,²¹ CdS,²² ZnS,²³ and ZnSe,²⁴ which possess both wurtzite and zinc blende polytypes without exception. The origin of such a WZ/ZB admixture is usually believed to be the low energy difference between the two lattice structures and the low interfacial energy between them. The present case provides another example, but the first report for such a phase admixture was in the MnS system. Note that all of the nanorods have larger WZ regions than ZB regions, which suggests the relatively higher stability of WZ over that of ZB in the present synthesis condition, although both phases are metastable polymorphs. It is necessary to mention that, according to the standard XRD patterns of WZ

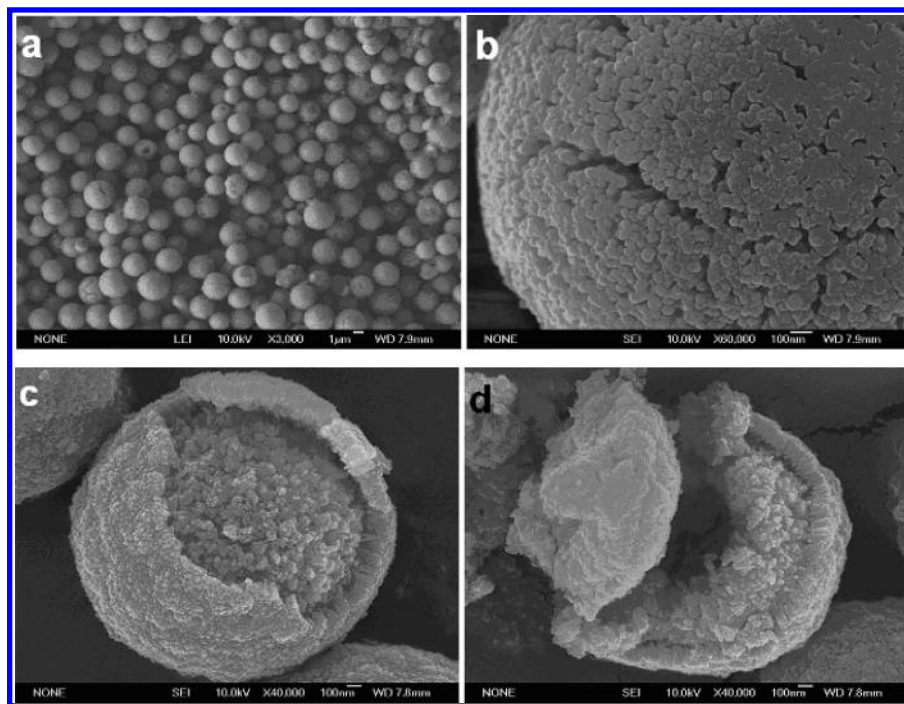


Figure 2. FESEM images of MnS microspheres.

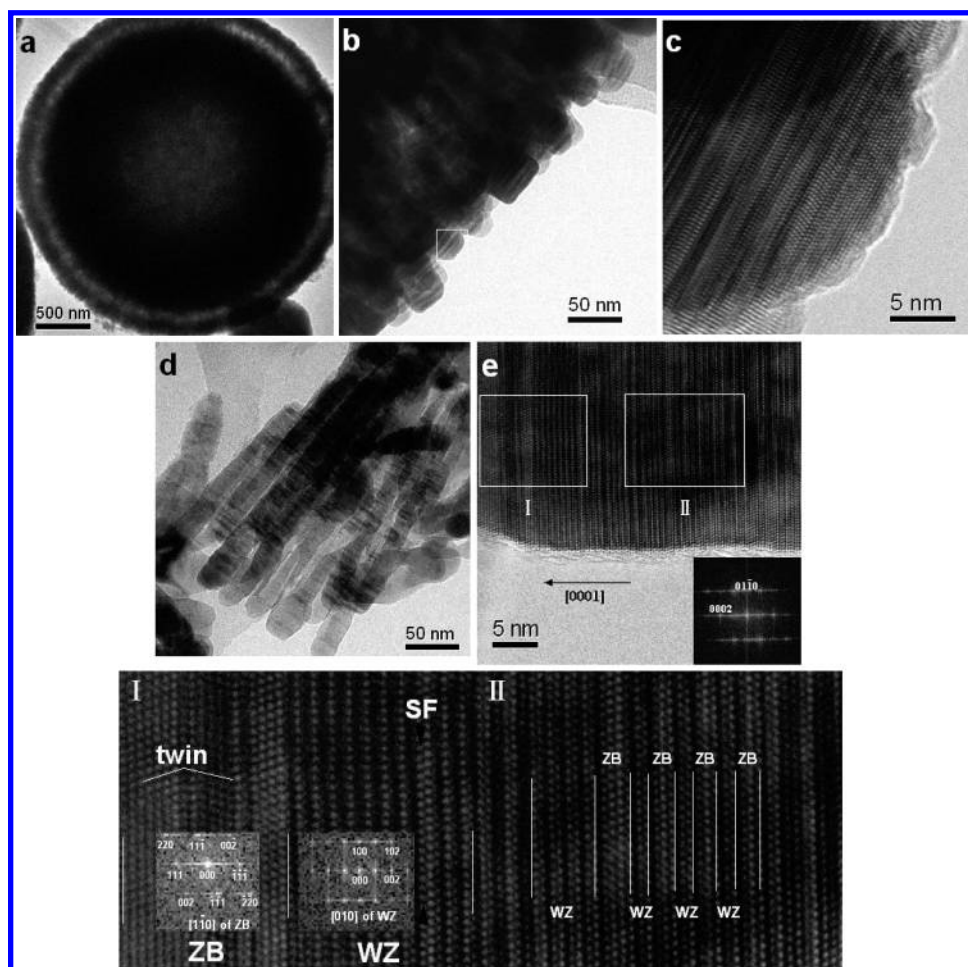


Figure 3. (a) TEM micrograph of a MnS microsphere. (b) TEM micrograph of the nanorod arrays in the shell of a microsphere. (c) HRTEM image from the top region of a nanorod (the squared region in (b)). (d) TEM micrograph of a bundle of nanorods broken off from the sphere. (e) HRTEM image of an individual broken nanorod; the inset is its corresponding FFT pattern. Parts I and II of (e) are the enlarged HRTEM images of the corresponding rectangular regions; the insets in I are FFT patterns from the ZB and WZ areas, respectively.

and ZB MnS (JCPDS No. 40-1289 and 40-1288, respectively), the WZ phase exhibits more diffraction peaks than its ZB

counterpart and all the main peaks of ZB locate almost at the same positions as those of WZ (see Supporting Information),

which explains why the XRD pattern (Figure 1) from the MnS product seems to exhibit only the WZ phase.

In particular, it is predicted by theory that the band gap difference between the two phases would make the WZ/ZB/WZ structures exhibit the features of a quantum well.²⁵ Carrier localization in the regions exhibiting quantum well features is expected to affect the electronic and transport properties. For a p-type semiconductor like MnS, the zinc blende well regions will behave like trap centers to the minority carriers (electrons) but like diffusion barriers to the majority carriers (holes). Furthermore, for the homomaterial heterostructure, both conduction and valence bands in the WZ structure are higher than those for the ZB counterparts, leading to the type II (staggered) band alignment.²⁶ As a result, the electrons tend to be confined to the ZB region, whereas the holes are kept to the WZ region. Such a charge separation would certainly affect the carrier recombination and thus the material photoluminescence, to some extent. Therefore, the unusual charge separation properties could find application in photovoltaic and photoconduction fields, for this type of heterostructure-induced longer decay lifetime would favor the carrier transfer before recombination occurs.

Conclusions

We provide the following summarizing points: (1) High yields of MnS microspheres with novel hierarchical structures were prepared through a simple solvothermal method. (2) The microspheres combine the hollow interior feature with a shell nanorod array characteristic. In particular, each nanorod contains a WZ/ZB phase admixture with a large amount of stacking faults/twins. (3) The alternation of WZ and ZB along the growth direction of the nanorod enables them to exhibit the features of a quantum well. In addition, the MnS WZ/ZB phase admixture structure could be regarded as a type II homomaterial heterostructure. All of these points imply that the synthesized novel structure has great potential for specific photoelectrical applications.

Acknowledgment. This work was supported by a project of the Nano-molecular Functional Materials of Fujian Province, China (2005HZ01-1), and the grants of the Natural Science Foundation of Fujian (A0320001, Z0513025).

Supporting Information Available: Comparison of Standard XRD patterns for WZ/ZB MnS. This material is available free of charge via the Internet at <http://pubs.acs.org>.

References and Notes

- (1) Caruso, F. *Adv. Mater. (Weinheim, Ger.)* **2001**, *13*, 11.
- (2) Dinsmore, A. D.; Hsu, M. F.; Nikolaides, M. G.; Marquez, M.; Bausch, A. R.; Weitz, D. A. *Science* **2002**, *298*, 1006.
- (3) Wang, Z.; Daemen, L. L.; Zhao, Y.; Zha, C. S.; Downs, R. T.; Wang, X.; Wang Z. L.; Hemley, R. J. *Nat. Mater.* **2005**, *4*, 922.
- (4) Xu, A.; Yu, Q.; Dong, W.; Antonietti, M.; Cölfen, H. *Adv. Mater. (Weinheim, Ger.)* **2005**, *17*, 2217.
- (5) Kumar, N.; Dorfman, A.; Hahn, J. J. *Nanosci. Nanotechnol.* **2005**, *5*, 1915.
- (6) Yang, H. G.; Zeng, H. C. *J. Phys. Chem. B* **2004**, *108*, 3492.
- (7) Mayers, B.; Jiang, X.; Sunderland, D.; Cattle, B.; Xia, Y. *J. Am. Chem. Soc.* **2003**, *125*, 13364.
- (8) Cheng, Y.; Wang, Y.; Chen, D.; Bao, F. *J. Phys. Chem. B* **2005**, *109*, 794.
- (9) Chen, J.; Saeki, F.; Wiley, B. J.; Cang, H.; Cobb, M. J.; Li, Z.; Au, L.; Zhang, H.; Kimmey, M. B.; Li, X.; Xia, Y. *Nano Lett.* **2005**, *5*, 273.
- (10) Liu, B.; Zeng, H. C. *J. Am. Chem. Soc.* **2004**, *126*, 8124.
- (11) Liu, B.; Zeng, H. C. *J. Am. Chem. Soc.* **2004**, *126*, 16744.
- (12) Yang, J.; Qi, L.; Lu, C.; Ma, J.; Cheng, H. *Angew. Chem., Int. Ed.* **2005**, *44*, 598.
- (13) Gunshor, R. L.; Nurmikko, A. V. *Semiconductors and Semimetals*; Academic: New York, 1997.
- (14) Petrakovskii, G. A.; Ryabinkina, L. I.; Kiselev, N. I.; Velikanov, D. A.; Bonina, A. F.; Abramova, G. M. *JETP Lett. (Engl. Trans.)* **1999**, *69*, 949.
- (15) Lu, J.; Qi, P.; Peng, Y.; Meng, Z.; Yang, Z.; Yu, W.; Qian, Y. *Chem. Mater.* **2001**, *13*, 2169.
- (16) An, C.; Tang, K.; Liu, X.; Li, F.; Zhou, G.; Qian, Y. *J. Cryst. Growth* **2003**, *252*, 575.
- (17) Biswas, S.; Kar, S.; Chaudhuri, S. *J. Cryst. Growth* **2005**, *284*, 129.
- (18) Zheng, Y.; Cheng, Y.; Wang, Y.; Zhou, L.; Bao, F.; Jia, C. *J. Phys. Chem. B* **2006**, *110*, 8284.
- (19) Kudara, S.; Carbone, L.; Casula, M. F.; Cingolani, R.; Falqui, A.; Snoeck, E.; Parak, W. J.; Manna, L. *Nano Lett.* **2005**, *5*, 445.
- (20) Salzemann, C.; Urban, J.; Lisiecki, I.; Pileni, M. P. *Adv. Funct. Mater.* **2005**, *15*, 1277.
- (21) Protasenko, V. V.; Hull, K. L.; Kuno, M. *Adv. Mater. (Weinheim, Ger.)* **2005**, *17*, 2942.
- (22) Murray, C. B.; Norris, D. J.; Bawendi, M. G. *J. Am. Chem. Soc.* **1993**, *115*, 8706.
- (23) Ma, C.; Moore, D.; Li, J.; Wang, Z. L. *Adv. Mater. (Weinheim, Ger.)* **2003**, *15*, 228.
- (24) Li, Q.; Gong, X.; Wang, C.; Wang, J.; Ip, K.; Hark, S. *Adv. Mater. (Weinheim, Ger.)* **2004**, *16*, 1436.
- (25) Yan, Y.; Dalpian, G. M.; Al-Jassim, M. M.; Wei, S. *Phys. Rev. B: Condens. Matter Mater. Phys.* **2004**, *70*, 193206.
- (26) Kim, S.; Fisher, B.; Eisler, H.; Bawendi, M. *J. Am. Chem. Soc.* **2003**, *125*, 11466.